ChemComm

Accepted Manuscript

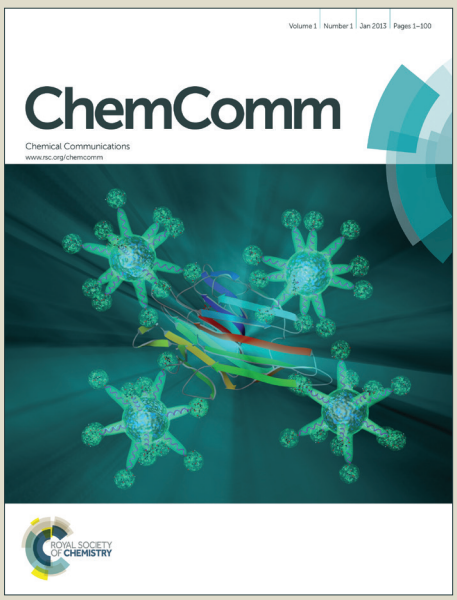

ROYAL SOCIETY OF CHEMISTRY

www.rsc.org/chemcomm

Cite this: DOI: 10.1039/c0xx00000x

www.rsc.org/xxxxxx

Communication

Organic nanoparticles with aggregation-induced emission for tracking bone marrow stromal cell in the rat ischemic stroke model

Kai Li,[‡a] Mie Yamamoto,[‡c,d] Su Jing Chan,[c] Mun Yee Chiam,[d] Wei Qin,[e] Peter Tsun Hon Wong,*[c] Evelyn K.F. Yim,*[d,f,g] Ben Zhong Tang[e,h] Bin Liu*[a,b]

Received (in XXX, XXX) Xth XXXXXXXXX 20XX, Accepted Xth XXXXXXXXX 20XX
DOI: 10.1039/b000000x

Organic nanoparticles (NPs) with aggregation-induced emission (AIE) have been successfully used for tracking bone marrow-derived mesenchymal stromal cells (BMSCs) in rats with ischemic stroke, highlighting the great potentials of such fluorescent NPs in understanding the fate of transplanted stem cells for cell-based therapies.

Stroke is the second most common cause of death and a leading cause of long-term disability worldwide,[1] which is predicted to intensify with the aging of population. Ischemic stroke accounts for 80% of all types of strokes.[2] Although mortality rate associated with stroke has declined with the advent of antithrombosis treatment,[3] only a small portion of ischemic patients can benefit from antithrombotic therapy because the thrombolytic agent (tissue plasminogen activator) has to be administered within a few hours upon the onset of stroke.[4] In addition to the narrow therapeutic time window, about half of the patients who received thrombolytic treatment showed little or no improvement in functional outcome.[5] Alternatively, cell-based therapy has emerged as an experimental therapeutic approach that may provide a longer time window of opportunity for treatment in acute stroke.[6] Among a variety of cells used for stroke treatment, bone marrow-derived stromal cells (BMSCs) have advantages as donor sources for regenerative medicine because they could be harvested from the patients themselves and the ethical dilemmas of using embryonic stem cells (ESCs) are thus avoided.[7] BMSCs are known as promising cell sources for ischemic stroke treatment through migration toward the cerebral infarct to promote functional recovery.[8] Despite these promising progress, cell therapies face significant challenges in realizing clinical practice because there are fundamental gaps in understanding the cell fate upon transplantation and the mechanism of their ability to promote stroke rehabilitation. As a result, effective cell labelling strategies are essential to allow tracking of the survival, migration, transformation and function of transplanted cells.

In comparison to various imaging techniques,[9] fluorescence imaging techniques show advantages in terms of better manoeuvrability, higher spatiotemporal resolution and more versatile imaging agents with good biocompatibility that carry no radioactive risk.[10] Currently, both direct and indirect approaches have been demonstrated for noninvasive cell labelling.[11] Indirect labelling strategies (e.g., introducing green fluorescent protein or luciferase into target cells), on one hand, could achieve long-term monitoring of gene-transfected cells; on the other hand, they require sophisticated gene transfection procedures which could induce disruption to normal cell functions.[12] Additionally, safety issues are a primary concern when viral vectors are used for transfection (e.g., immunogenicity of viral vectors and haphazard integration of viral genes into the host genome).[13] Non-viral vectors are not a good alternative as previous studies have shown that they give very low transfection efficiency in BMSCs (~20 to 30%).[14] As compared to indirect labelling, direct labelling approaches generally offer higher labelling efficiency without gene transfection. Currently, the commercially available quantum dot (QD)-based labelling kits are the most promising fluorescent agents for direct labelling and long-term cell tracking.[15] Unfortunately, QDs contain intrinsically toxic heavy metal components and a recent study has shown that QD-based labelling kits were found to compromise transplanted stem cell function and give false signals during cell therapeutic treatment *in vivo*.[16]

To date, efforts have been made to develop organic fluorescent NPs as promising alternatives to QDs with lower cytotoxicity and better performance.[17] We have previously reported a new generation of cell-penetrating peptide-functionalized fluorescent nanoparticles (NPs) with aggregation-induced emission (AIE) characteristics and improved tracking ability over the commercial Qtracker® in long-term cancer cell tracking.[18] The excellent tracking ability of such AIE NPs in cancer cell studies motivates us to investigate their performance in stem cell tracking with the hope to understand the fate of transplanted cells, which will help unveil the limitations of current stem cell therapy (e.g., engraftment and poor survival of delivered cells).[19] In this contribution, we report the application of AIE NPs for tracking of transplanted BMSCs in rats subjected to experimental ischemic stroke. The cells showed a labelling efficiency of ~100% even after subculturing in fresh culture medium for 9 days *in vitro*. An obvious accumulation of labelled BMSCs at the site of ischemic injury was observed on day 7 following transplantation. The low cytotoxicity, excellent cell tracking ability and high brightness of Tat-AIE NPs enable clear visualization of preferential accumulation of BMSCs at the cerebral injury tissue, suggesting that Tat-AIE NPs could be an invaluable tool in investigating cell fate following cell transplantation therapy.

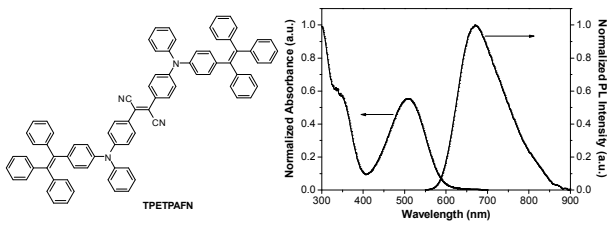

Fig. 1 The chemical structure of TPETPAFN, and UV-Vis absorption and photoluminescence spectra of Tat-AIE NPs in water suspension (λ_{ex} = 512 nm).

The AIE NPs with surface maleimide groups were synthesized according to literature through a nanoprecipitation method.[20] The mixture of 1,2-distearoyl-*sn*-glycero-3-phosphoethanolamine-*N*-[methoxy(polyethylene glycol)-2000] (DSPE-PEG$_{2000}$) and its derivative, DSPE-PEG$_{2000}$-Malaimide, were employed as a biocompatible matrix to encapsulate the AIE fluorogen to yield AIE NPs with abundant surface maleimide groups for further modification. The obtained water suspension of AIE NPs was then mixed with a cysteine-modified cell penetrating peptide (RKKRRQRRRC), derived from HIV-1 transactivator of transcription (Tat) protein. The surface maleimide groups of AIE NPs reacted with the thiol groups at the C-terminus of Tat peptide and afforded the Tat-AIE NPs. The obtained Tat-AIE NPs have excellent colloidal stability in water suspension upon storage at 4 ºC for 6 months without obvious precipitation observed. The average size of Tat-AIE NPs is 35 ± 3 nm, determined by laser light scattering. The quantum yield of NPs is 26% in water, measured using 4-(dicyanomethylene)-2-methyl-6-(p-dimethylaminostyryl)-4H-pyran in methanol as standard (Φ_F = 43%).[21] The water suspension of NPs shows a maximum absorption at 512 nm with intense emission above 650 nm, which is beneficial to tissue imaging (Fig. 1).

BMSCs were isolated from rat bone marrow and cultured *in vitro* up to passage 5 (P5). As a heterogeneous population of mesenchymal stem cells and progenitor cells can be proliferated from BMSCs after continuous *in vitro* culturing, the P5 cells were then analyzed through immunofluorescence staining to study the mesenchymal stem cell markers (CD29 and CD90). The hematopoietic marker, CD45, was used to screen cells of non-mesenchymal lineage. Biotinylated anti-CD29 monoclonal antibody (mAb), biotinylated anti-CD45 mAb, and anti-CD90 mAb were used for incubation with P5 BMSCs, respectively, followed by further staining with Alexa Fluor® 488 streptavidin or Alexa Fluor® 488 antibody conjugates to facilitate fluorescence imaging. As shown in Fig. S1 in the Supplementary Information (SI), bright green fluorescence could be observed from P5 BMSCs incubated with biotinylated anti-CD29 mAb/Alexa Fluor® 488 streptavidin and cells incubated with anti-CD90 mAb/Alexa Fluor® 488 antibody. These results indicate that P5 BMSCs are strongly positive for mesenchymal cell markers. In contrast, these cells were barely immuno-reactive with hematopoietic marker, CD45 (Fig. S1d). Flow cytometry analysis, employed to assess immunofluorescence staining results, revealed that 89.3% of P5 BMSCs are doubly positive for CD29 and CD90 while only 3.1% is CD45 positive. As a result, P5 BMSCs are a homogeneous population of cells with mesenchymal properties.

The cell uptake of Tat-AIE NPs was first investigated upon incubation with P5 BMSCs for 4 h at 37 °C and the results are shown in Fig. S2 in the SI. Figs. S2a and S2b clearly indicate that the Tat-AIE NPs are distributed in cell cytoplasm without serious aggregation to emit intense fluorescence with a labelling efficiency of ~100%. Under the same experimental conditions, only very weak fluorescent signal from cells is detected when AIE NPs without surface Tat peptide were used for incubation (Fig. S2c). These results suggest that the Tat peptide on Tat-AIE NP surface is essential to facilitate efficient internalization of the NPs into living cells. After incubation with 2, 4 and 6 nM Tat-AIE NPs for 48 h, the metabolic viability of BMSCs remained above 90%, as determined by the methylthiazolyldiphenyltetrazolium bromide (MTT) assays (Fig. S3 in the SI). The high living cell internalization efficiency and the low cytotoxicity of Tat-AIE NPs to BMSCs should make them suitable for long-term cell tracking studies both *in vitro* and *in vivo*.

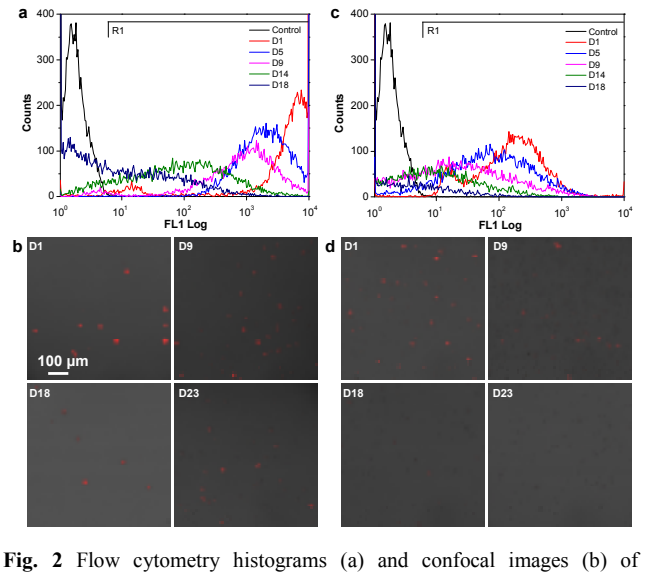

Fig. 2 Flow cytometry histograms (a) and confocal images (b) of suspended BMSCs after incubation with 2 nM Tat-AIE NPs at 37 °C overnight and then subcultured for designated days. The data for BMSCs treated with Qtracker® 655 are shown in (c) and (d). The untreated BMSCs were used as the control for flow cytometry analysis (λ_{ex} = 488 nm, 680/30 nm bandpass filter). Positivity threshold: <0.5% false positives (gating based on the control). The confocal images were taken under excitation at 514 nm (~1 mW) with a 550–800 nm bandpass filter. All images share the same scale bar.

The *in vitro* cell tracking ability of Tat-AIE NPs was studied using commercial Qtracker® 655 labelling kit as the reference. After incubation with 2 nM Tat-AIE NPs or Qtracker® 655 overnight at 37 °C, the labelled cells were detached and subcultured continuously for different time intervals to record the fluorescence profiles using flow cytometry (λ_{ex} = 488 nm, 680/30 nm bandpass filter, n = 10,000). As shown in Fig. 2a and Fig. 2c, the average fluorescence intensity of Tat-AIE NP-labelled cells is obviously higher as compared to that of Qtracker® 655-labelled ones. Upon subculturing for one day, the labelling efficiencies of BMSCs incubated with Tat-AIE NPs and Qtracker® 655 are 99.8% and 98.8%, respectively. The labelling efficiency of Tat-AIE NP-treated cells remains 99.0 % after 9 days and 51.0% of

the cells are considered to be labelled after 18-day subculture. On the other hand, only 61.4% and 10.4% of Qtracker® 655-treated cells remain efficiently labelled at day 9 and day 18, respectively. The results clearly prove that Tat-AIE NPs have dramatically superior BMSC tracking ability over Qtracker® 655 in *in vitro* study. Confocal images of the BMSCs were further obtained after flow cytometry tests. Both Tat-AIE NP and Qtracker® 655-labelled cells show intense fluorescent signals at day 1 (Figs. 2c and 2d), due to the efficient labelling efficiency and high brightness of the probes. Almost all the cells labelled with Tat-AIE NPs emit fluorescence at day 9 and intense signal is visible even at day 23. On the contrary, only very weak fluorescence from some cells labelled with Qtracker® 655 is distinguishable at day 18 under the same experimental conditions. Furthermore, 3D color-coded projection of confocal images of the suspended BMSCs is shown in Fig. S4, indicating that the AIE NPs are mainly localized in cell cytoplasm.

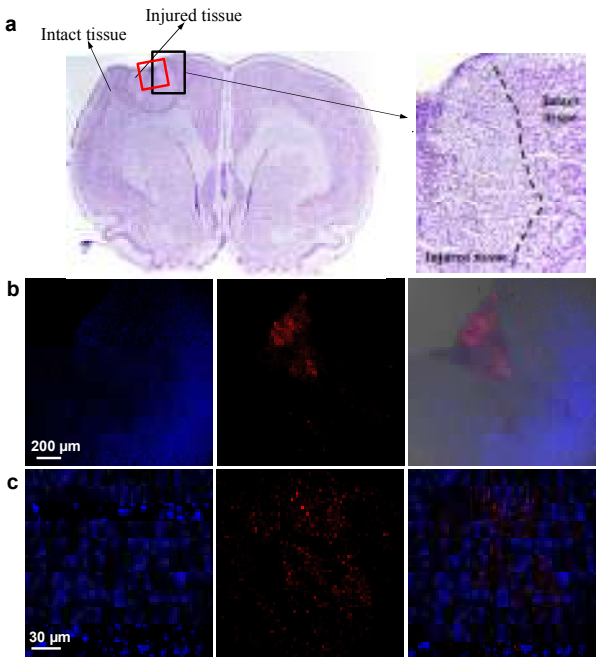

Fig. 3 (a) Thionin staining of brain tissue collected from rat with ET-1 induced ischemic stroke after 7 days upon BMSC transplantation. (b) Fluorescence images of the lesion site in sectioned brain tissue collected from the rat at day 7 post injection of Tat-AIE NP-labelled BMSCs. From left to right: fluorescence image of DAPI channel (420-500 nm), fluorescence image of Tat-AIE NP channel (600-800 nm) and the overlay image of fluorescence/transmission images (λ_{ex} = 405 nm). (c) Fluorescence images of the lesion site under a high magnification. From left to right: fluorescence image of DAPI channel (420-500 nm), fluorescence image of Tat-AIE NP channel (600-800 nm), and the overlay image. The red box in (a) indicates the region for confocal images in (b).

Experimental stroke was induced in rat by unilateral topical application of endothelin-1 (ET-1, 5μl, 250pmol) on the exposed middle cerebral artery (0.5 mm posterior and 2.5 mm anterior to bregma). As a potent vasoconstrictor, ET-1 occludes the artery and thus induces ischemic stroke.[22] Tat-AIE dot-labelled P5 BMSCs were then infused into internal carotid artery (ICA) of the rats at 24 h post stroke. The rats were perfused with phosphate buffered saline (PBS) 7 days after BMSC transplantation and the brain was collected for analysis. Brain sections (40 μm thick) were stained with thionin to reveal the infarct region. As shown in the Fig. 3a, the circled area (dash line) in the left hemisphere of brain administrated with ET-1 clearly shows cell loss when compared to the intact tissue,[23] indicating the successful creation of ischemic stroke model.

The brain tissue sections were then stained with 4',6-diamidino-2-phenylindole (DAPI) and imaged under confocal microscopy to study the localization and engraftment of transplanted BMSCs. As shown in Fig. 3b, the blue fluorescence indicates DAPI stained nuclei in brain tissue and red fluorescent signal is from BMSCs labelled with Tat-AIE NPs. It can be clearly seen that a large number of Tat-AIE NP-treated BMSCs accumulate at the injured tissue but not the intact tissue, suggesting that BMSCs have the ability to migrate to the site of cerebral injury.[24] Images in Fig. 3c clearly show the BMSC accumulation in the lesion site under a higher magnification. These results further confirm that the internalization of Tat-AIE NPs in BMSCs does not prohibit the migration of therapeutic cells to the lesion site, indicating the great potential of such Tat-AIE NPs as effective fluorescent trackers in cell therapy studies.

In summary, we demonstrated the application of organic fluorescent Tat-AIE NPs for long-term tracking of BMSCs with mesenchymal property using an ischemic stroke model. The Tat-AIE NPs were found to be able to label rat BMSCs with high labelling efficiency through simple incubation. After 18 days continuous subculture, 51.0% of the Tat-AIE NP-treated cells remain efficiently labelled while only 10.4% of the Qtracker® 655-treated cells have fluorescence. Upon transplantation into a ET-1 stroke model, *ex vivo* analysis reveals that the Tat-AIE NP-labelled P5 BMSCs could preferentially accumulate to the injured tissue but not the intact ones, suggesting that the internalization of Tat-AIE NPs did not affect the migration ability of BMSCs to stroke site. Further evaluation of the cell fate (e.g., viability, proliferation and differentiation) after migration to the lesion site will be carried out to understand the behaviour and function of BMSCs in ischemic strokes. In addition, incorporation of radiative agents to the AIE NPs could also afford dual-modality imaging probes with both high spatial and temporal resolutions, which is desired for real-time *in vivo* monitoring of the migration and function of transplanted BMSCs in brain tissues.

The authors are grateful to A*STAR Joint Council Office and Institute of Materials Research and Engineering of Singapore (IMRE/12-8P1103, IMRE/13-8P1104, IMRE/14-8P1110), the Singapore National Research Foundation (R279-000-390-281), Singapore Ministry of Defence (R279-000-340-232), the National University of Singapore (R279-000-415-112), National Research Foundation Singapore under the Competitive Research Programme (NRF-CRP003-2008-01), the Research Center of Excellence programme administered by the Mechanobiology Institute of Singapore, the Research Grants Council of Hong Kong (HKUST2/CRF/10 and N_HKUST620/11) and Guangdong Innovative Research Team Program (201101C0105067115) for financial support.

Notes and references

[a]*Institute of Materials Research and Engineering, A*STAR, 3 Research Link, Singapore 117602*

[b]Department of Chemical and Biomolecular Engineering, National University of Singapore, 4 Engineering Drive 4, Singapore 117585. Fax: +65-67791936; Tel: +65-65168049; E-mail: cheliub@nus.edu.sg
[c]Department of Pharmacology, Center for Translational Medicine, Yong Loo Lin School of Medicine, National University Health System, National University of Singapore, Singapore 117597; E-mail: peter_wong@nuhs.edu.sg
[d]Department of Biomedical Engineering, National University of Singapore, 9 Engineering Drive 1, Singapore 117575; E-mail: eyim@nus.edu.sg
[e]Department of Chemistry, Division of Biomedical Engineering, Institute for Advanced Study, State Key Laboratory of Molecular Neuroscience, and Institute of Molecular Functional Materials, The Hong Kong University of Science & Technology, Clear Water Bay, Kowloon, Hong Kong, China
[f]Mechanobiology Institute Singapore, National University of Singapore, 5A Engineering Drive 1, Singapore 117411
[g]Department of Surgery, Yong Loo Lin School of Medicine, National University of Singapore, NUHS Tower Block, IE Kent Ridge Road, Singapore 119228
[h]SCUT-HKUST Joint Research Laboratory, Guangdong Innovative Research Team, State Key Laboratory of Luminescent Materials and Devices, South China University of Technology, Guangzhou, China, 510640

† Electronic Supplementary Information (ESI) available: experimencal sections, immunofluorescence imaging of P5 BMSCs, confocal images of BMSCs after incubation with NPs, cytotoxicity of Tat-AIE NPs and 3D confocal image of BMSCs. See DOI: 10.1039/b000000x/
‡These authors contributed equally to this work.

1 S. M. Davis and G. A. Donnan, *N. Engl. J. Med.*, 2012, **366**, 1914.
2 H. S. Kirshner, *J. Neurl. Sci.*, 2009, **279**, 1.
3 M. Lalancette-Hebert, D. Phaneuf, G. Soucy, Y. C. Weng and J. Kriz, *N. Engl. J. Med.*, 2009, **132**, 940.
4 (a) A. Eissa, I. Krass and B. V. Bajorek, *J. Clin. Pharm. Ther.*, 2012, **37**, 620; (b) The National Institute of Neurological Disorders and Stroke rt-PA Stroke Study Group, *N. Engl. J. Med.*, 1995, **333**, 1581.
5 (a) O. Adeoye, R. Hornung, P. Khatri and D. Kleindorfer, *Stroke*, 2011, **42**, 1952; (b) N. Wahlgren, N. Ahmed, A. Dávalos, G. A. Ford, M. Grond, W. Hacke, M. G. Hennerici, M. Kaste, S. Kuelkens, V. Larrue, K. R. Lees, R. O. Roine, L. Soinne, D. Toni, G. Vanhooren and SITS-MOST investigators, *Lancet*, 2007, **369**, 275.
6 D. C. Hess and C. V. Borlongan, *Expert Rev. Neurother.*, 2008, **8**, 1193.
7 (a) L. Zhang, Y. Li, M. Romanko, B. C. Kramer and A. Gosiewska, *Brain Res.*, 2012, **1489**, 104; (b) Z. G. Zhang and M. Chopp, *Lancet Neurol.*, 2009, **8**, 491; (c) P. R. Sanberg, D. J. Eve, C. Metcalf and C. V. Borlongan, *Prog. Brain Res.*, 2012, **201**, 99.
8 (a) J. Chen, Y. Li, L. Wang, M. Lu, X. Zhang and M. Chopp, *J. Neurol. Sci.*, 2001, **189**, 49; (b) H. Shichinohe, S. Kuroda, S. Yano, K. Hida and Y. Iwasaki. *Brain Res*., 2007, **1183**, 138.
9 (a) X. Chen, D. Miranda-Nieves, J. A. Ankrum, M. E. Matthiesen, J. A. Phillips, I. Roes, G. R. Wojtkiewics, V. Juneja, J. R. Kultima, W. Zhao, P. K. Vemula, C. P. Lin, M. Nahrendorf and J. M. Karp, *Nano Lett.*, 2012, **12**, 4131; (b) N. Adonai, K. N. Nguyen, J. Walsh, M. Iyer, T. Toyokuni, M. E. Phelps, T. McCarthy, D. W. McCarthy and S. S. Gambhir, *Proc. Natl. Acad. Sci. U. S. A.*, 2002, **99**, 3030; (c) D. L. Kraitchman, M. Tatsumi, W. D. Gilson, T. Ishimori, D. Kedziorek, P. Walczak, W. P. Segars, H. H. Chen, D. Fritzges, I. Izbudak, R. G. Young, M. Marcelino, M. F. Pittenger, M. Solaiyappan, R. C. Boston, B. M. Tsui, R. L. Wahl and J. W. Bulte, *Circulation*, 2005, **112**, 1451; (d) J. V. Jokerst, C. Khademi and S. S. Gambhir, *Sci. Transl. Med.*, 2013, **5**, 177ra35.
10 (a) V. R. Kondepati, H. M. Heise and J. Backhaus, *J. Anal. Bioanal. Chem.*, 2008, **390**, 125; (b) L. Fass, *Mol. Oncol.*, 2008, **2**, 115.
11 M. F. Kircher, S. S. Gambhir and J. Grimm, *Nat. Rev. Clin. Oncol.*, 2011, **8**, 677.
12 E. Dellambra, G. Pellegrini, L. Guerra, G. Ferrari, G. Zambruno, F. Mavilio and M. De Luca, *Hum. Gene Ther.*, 2000, **11**, 2283.
13 B. A. Clements, J. Bai, C. Kucharski, L.-L. Farrell, A. Lavasanifar, B. Ritchie, A. Ghahary and H. Uludag. *Biomacromolecules*, 2006, **7**, 1481.
14 B. A. Clements, V. Incani, C. Kucharski, A. Lavasanifar, B. Ritchie and H. Uludağ, *Biomaterials*, 2007, **28**, 4693.
15 (a) L. Xin, R. U. Lukacs, D. A. Lawson, D. Cheng and O. N. Witte, *Stem Cells*, 2007, **25**, 2760; (b) S. Lin, X. Xie, M. R. Patel, Y.-H. Yang, Z. Li, F. Cao, O. Gheysens, Y. Zhang, S. S. Gambhir, J. H. Rao and J. Wu, *BMC Biotechnol.*, 2007, **7**, 67.
16 K. M. Dupont, K. Sharma, H. Y. Stevens, J. D. Boerckel, A. J. Garcia and R. E. Guldberg. *Proc. Natl. Acad. Sci. U. S. A.*, 2009, **107**, 3305.
17 (a) D. Ding, K. Li, B. Liu and B. Z. Tang, *Acc. Chem. Res.*, 2013, **46**, 2441; (b) L. Feng, C. Zhu, H. Yuan, L. Liu, F. Lv and S. Wang, *Chem. Soc. Rev.*, 2013, **42**, 6620; (c) S. Luo, E. Zhang, Y. Su, T. Cheng and C. Shi, *Biomaterials*, 2011, **32**, 7127; (d) K. Li and B. Liu, *J. Mater. Chem.*, 2012, **22**, 1257.
18 (a) K. Li, W. Qin, D. Ding, N. Tomczak, J. Geng, R. Liu, J. Liu, X. Zhang, H. Liu, B. Liu and B. Z. Tang, *Sci. Rep.*, 2013, **3**, 1150; (b) K. Li, Z. Zhu, P. Cai, R. Liu, N. Tomczak, D. Ding, J. Liu, W. Qin, Z. Zhao, Y. Hu, X. Chen, B. Z. Tang and B. Liu, *Chem. Mater.*, 2013, **25**, 4181; (c) W. Qin, K. Li, G. Feng, M. Li, Z. Yang, B. Liu and B. Z. Tang, *Adv. Funct. Mater.*, 2014, **24**, 635.
19 M. J. Cooke, K. Vulic and M. S. Schoichet, *Soft Matter.*, 2010, **6**, 4988.
20 (a) D. Ding, C. C. Goh, G. Feng, Z. Zhao, J. Liu, R. Liu, N. Tomczak, J. Geng, B. Z. Tang, L. G. Ng and B. Liu, *Adv. Mater.*, 2013, **25**, 6083; (b) K. Li, D. Ding, C. Prashant, W. Qin, C. T. Yang, B. Z. Tang and B. Liu, *Adv. Healthcare Mater.*, 2013, **12**, 1600; (c) G. Feng, C. Y. Tay, Q. X. Chui, R. Liu, N. Tomczak, J. Liu, B. Z. Tag, D. T. Leong and B. Liu, *Biomaterials*, 2014, **35**, 8669; (d) K. Li and B. Liu, *Chem. Soc. Rev.*, 2014, **43**, 6570.
21 J. M. Drake, M. L. Lesiecki and D. M. Camaioni, *Chem. Phys. Lett.*, 1985, **113**, 530.
22 M. D. Binder, N. Hirokawa and U. Windhorst, *Encyclopedia of Neuroscience*, Springer, 2009.
23 (a) G. Tsenov, A. Mátéffyová, P. Mareš, J. Otáhal and H. Kubová, *Epilepsia*, 2007, **48**, 7; (b) P. Wolinski and A. Glabinski, *Mediators Inflamm.*, 2013, **2013**, 727189.
24 (a) L. H. Shen, Y. Li, J. Chen, A. Zacharek, Q. Gao, A. Kapke, M. Lu, K. Raginski, P. Vanguri, A. Smith and M. Chopp, *J. Cereb. Blood Flow Metab.*, 2007, **27**, 6; (b) D. M. Seyfried, Y. Han, D. Yang, J. Ding, L. H. Shen, S. Savant-Bhonsale and M. Chopp, *J. Neurosurg.*, 2010, **112**, 329.